Computer Simulation of the Inrush Current of Frequency Converter during Initial Start-Up

MIKHAIL PUSTOVETOV
Department of Electrical and Electronics Engineering,
Don State Technical University,
344000, Rostov region, Rostov-on-Don, Gagarin sq., 1,
RUSSIA

Abstract: - The paper presents a theoretical study using computer simulation of the influence of DC voltage link parameters of a frequency converter on the value of current consumed by the converter from the grid (input current). Frequency converters of different rated powers are considered. The presence of inductance in DC voltage link should be recognized as very useful and desirable for lower-power and medium-power frequency converters, since it has a strong limiting effect on the peak and amplitude values of the input current consumed by converter, and also has a beneficial effect on the harmonic composition of the input current, improving the convertor's electromagnetic compatibility.

Key-Words: - input current, capacitor charging process, frequency converter, L-shaped filter of DC link, induction motor, start-up, precharge resistance.

Received: June 4, 2024. Revised: November 13, 2024. Accepted: December 6, 2024. Published: December 31, 2024.

1 Introduction

An automated electric drive using induction motors (IM) powered by frequency converters (FC) is widely used in various industries and transport. It seems that its characteristics are well known. However, during operation, questions sometimes arise, the answers to which can only be given by conducting experiments with specific equipment. Unfortunately, in production conditions, a set of devices for the appropriate measurements is not always available. In addition, the production technology does not always allow for the possibility of conducting experiments. A contemporary effective replacement for a physical experiment can be a computational experiment, that is, simulation using an adequate mathematical model of the object of study, [1], [2], [3], [4], [5], [6], [7], [8], [9]. Unfortunately, we have to state that accurate and sufficient data for constructing an adequate mathematical model of the FC are not always available: not everything is specified in the documentation, and not every owner of FC is ready to disassemble it for identification of the parameters of components. Thus, when setting the parameters of the mathematical model, it is necessary to rely on the regularities characteristic of a number of FCs. For example, the power of the IM connected to the FC is known, but there is no data on the values of C_d and L_d - the parameters of the L-shaped filter in the DC link of the FC. Of course, in such a situation it is impossible to provide the customer with completely reliable simulation results, but knowing the approximate values of C_d and L_d, it is possible to obtain approximate results that do not contradict the physics of the processes and common sense. One of the characteristics of interest in practice is the value of the current consumed by the phase of the FC during its initial start-up (saying other words, inrush current, [10], [11]).

2 Problem Formulation

Several electric drives based on FCs and IMs are used at the confectionery factory. The total installed power of the IMs group (16 units) is about 9.3 kW (including IMs with rated powers of 0.37 kW, 0.75 kW, and 1.5 kW). Each IM is powered by an individual FC. The IMs group is energizing (turning on under uninterruptible power supply (UPS) output voltage) simultaneously. The specified load is powered by one UPS with a rated power of 20 kVA. The frequency start can be allowed simultaneously for no more than four IMs by the control system. A problem has been identified consisting of periodic failure of the transistors of the UPS output inverter. It is known that the maximum permissible continuous RMS current of the UPS is 40 A, and an overload RMS current of 200% withstand ability is guaranteed for 0.5 s (this corresponds to a current amplitude of 113.137 A). The purpose of the work is to determine the value of the total phase current consumed by the FCs group during initial start-up under the output voltage of UPS. Can this inrush the current value of the FCs group be dangerous for the UPS?

3 Problem Solution

Due to the fact that the management of the confectionery factory prohibited stopping the technological process to conduct experiments with the equipment, it was decided to use the computer simulation method.

All the FCs with a DC link considered in this case have an input diode rectifier implemented according to a 6-pulse bridge circuit; an L-shaped low-pass filter with an inductance L_d in the longitudinal branch and a capacitance C_d in the transverse branch; a transistor-based autonomous voltage source inverter (AVSI) implemented according to a bridge circuit (Figure 1). When the FC is turning-on under voltage, the initial charging of the capacitance C_d begins through the precharge resistance R, which is shunted after some time, sufficient for the voltage on the capacitor to reach a value close to the nominal value (for FCs of type SIMOVERT MASTERDRIVES in the output range from 2.2 kW to 37 kW it is factory preset the minimum DC link voltage 80 %, when pre-charging, which have to be achieved within a duration not more than 3 s [12]), by contactor K, through which C_d is finally charging, after which it is possible to begin supplying the AC voltage from the AVSI to load [13], [14]. Such a method of C_d pre-charging is adopted, for example, for FCs of types: SIEMENS SIMOVERT MASTERDRIVES [12], KEB COMBIVERT F4-C [15], ABB ACS-300 [16], VEDA VFD VF-51, VESPER EI-9011. The FC is powered from a symmetrical three-phase voltage source with a frequency of 50 Hz and an RMS line voltage of 380 V.

The author is aware of modern soft start-up techniques for inrush current limitations with controlled MOSFET transistors [10], [11], [17]. However, such devices are not considered in this paper, because when they are used, inrush currents are noticeably reduced.

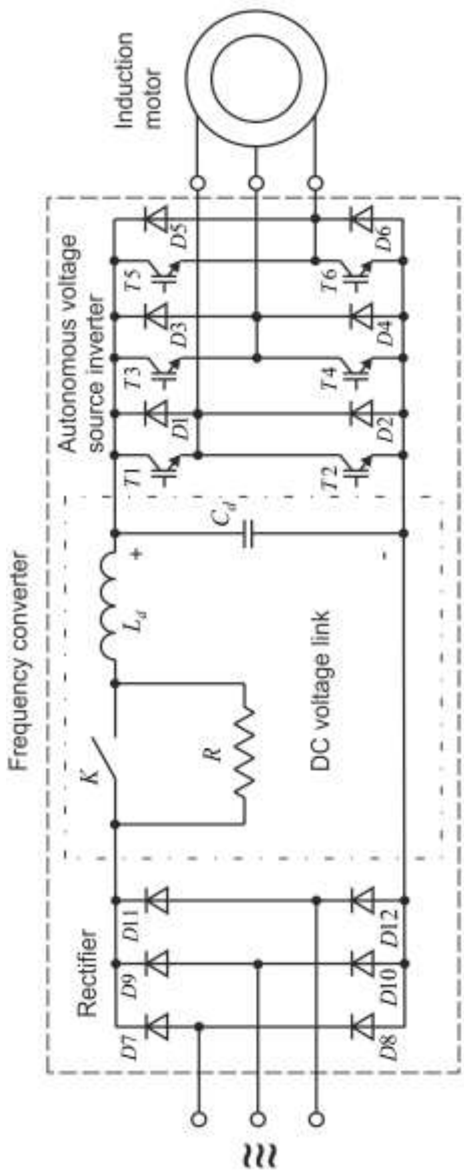

Fig. 1: Power section diagram of FC

In order to reasonably specify the values of C_d and L_d, the author attempted to generalize a number of data known to him from practice, as well as from catalogs [1] for FCs for input and output linear three-phase RMS voltages of 380 V. The results are presented in Figure 2 in the form of L_d values, mH, and specific C_d values, μF/kW. According to Figure 2(b), the arithmetic mean specific value of C_d is 322 μF/kW. Figure 2 shows the equations of the trend lines (dotted lines), as well as the reliability of the approximation of the specified specific parameter values by the trend line (marker points) R^2 is the coefficient of determination, indicating the extent to which the trend described by this equation explains the location of the initial points. An important starting point for selecting the DC link filter parameters is the ripple voltage value. Practically a reasonable amount of ripple voltage on the DC-bus in the single percent range would be acceptable, [18].

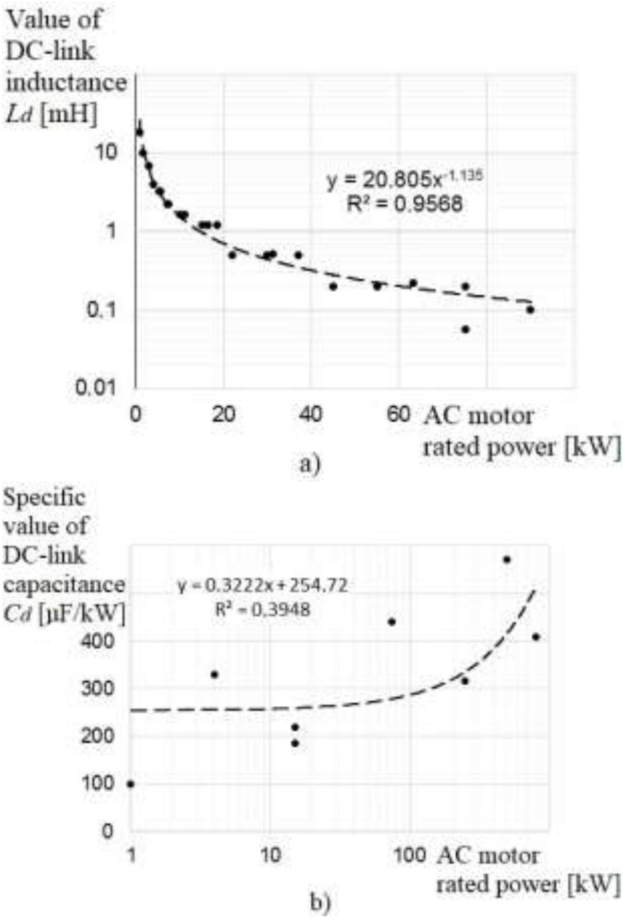

Fig. 2: Approximate dependencies of the parameters of the DC link of FC vs rated power of connected IM [1]: a) the value of L_d ; b) the specific value of C_d

Further results were obtained for the case of simulating the initial starting-up of the FC in the absence of an initial charge on C_d and the frequency start of an IM with a rated power of 1.5 kW with a shaft load of the fan or pump type.

The characteristics and parameters of the IM of type AEV 80 V2U2 are given in Table 1. Table 2 shows the characteristics and parameters of the L-shaped filter of FC and the capacitor charging unit adopted in the simulation. The simulation was carried out for two cases: when L_d is present in the DC link filter and when L_d is absent.

The simulation results for the input current consumed by the phase of FC are summarized in Table 3. The data in Table 3 provide an idea of the peak values of currents consumed from the UPS. Figure 3 shows the simulation results in the presence of L_d from the time moment of FC power supply being turned on until the IM reaches the steady-state operating mode at an output AVSI voltage frequency of 50 Hz.

Table 1. Characteristics and parameters of the AEV 80 V2U2 type IM used for the simulation

Name of characteristic or parameter	Units of measurement	Value
Rated shaft power	kW	1.5
Rated rotational speed	rpm	2909
Rated RMS linear voltage	V	380
Rated frequency	Hz	50
Stator winding phase resistance @ 75 ◦C	Ohm	5.63
Reduced (to stator) phase resistance of rotor winding @ 75 ◦C	Ohm	2.18
Stator winding phase leakage inductance	H	0.0112
Reduced (to stator) rotor winding phase leakage inductance	H	0.00703
Main inductance	H	0.3119
Iron loss resistance (resistance in the magnetization branch connected in parallel with the main inductance)	Ohm	996.6
IM shaft inertia (taking into account mechanism)	$kg \cdot m^2$	$36.6 \cdot 10^{-4}$

Figure 4 shows the initial fragment of the transient process from Figure 3. Figure 5 shows the same initial fragment of the transient process in time, but in the absence of L_d . The figures show the graphs: 1 - current consumed by the phase of the FC, A; 2 - DC link voltage (reduced by 20 times), V; 3 - frequency of the output voltage of the AVSI (changed by 0.6 times), Hz; 4 - rotational speed of the rotor of the IM (reduced by 100 times), rpm. Figure 6 and Figure 7 show the waveform of the current consumed by the phase of the FC obtained as a result of simulation, respectively, in the presence and absence of L_d .

Table 2. Characteristics and parameters of the FC

Name of characteristic or parameter	Units of measurement	Value
Capacitance C_d of the L-shaped filter	μF	400
Inductance L_d of the L-shaped filter (if any)	mH	10
Precharge resistance	Ohm	10
Delay in the start of closing the contactor shunting the precharge resistor from the time moment of voltage supply to the FC input	s	0.01
Duration of the contactor closure, shunting the precharge resistor	μs	1
Resistance of the shunting contactor in the opened state	MOhm	1
Resistance of the shunting contactor in the closed state	Ohm	0.001

Table 3. Simulation results for the input current consumed by phase of FC

Name of characteristic	Units of measurement	Value	
		with L_d	without L_d
Peak voltage across C_d terminals during charging	V	548.193	537.834
Peak inrush current when charging C_d through a precharge resistor	A	39.131	46.457
Peak inrush current during final charging of C_d through the contactor shunting the precharge resistor	A	-10.231	-134.207
Peak input current during the process of frequency acceleration of the IM	A	-12.758	49.775
Steady-state mode input current amplitude after completion of acceleration of the IM	A	7.348	44.089
Steady-state mode input current 1st harmonic amplitude after completion of acceleration of the IM	A	5.927	5.913
Steady-state mode input current THD after completion of acceleration of the IM (harmonics with frequencies up to 2000 Hz are taken into account)	%	7.340	13.056

Further simulation results are given for the case of the presence of L_d. The duration of the contactor closure, shunting the precharge resistor; the resistance of the shunting contactor in the opened state and the resistance of the shunting contactor in the closed state are taken everywhere to be the same as in Table 2. Table 4 contains information about the parameters and characteristics of the simulated FCs. Table 5 presents the input current consumed by the FC phase simulation results for IMs of different rated shaft power.

Table 4. Characteristics and parameters of the FC adopted during simulation

Name and units of characteristic or parameter	Value		
Rated power of the IM being connected, kW	0.37	0.75	7.5
Capacitance C_d of the L-shaped filter, μF	120	250	2400
Inductance L_d of the L-shaped filter, mH	18	18	2.2
Precharge resistance R, Ohm	20	15	3
Delay in the start of closing the contactor shunting the precharge resistor R from the time moment of voltage supply to the input of FC, s	0.005	0.01	0.01

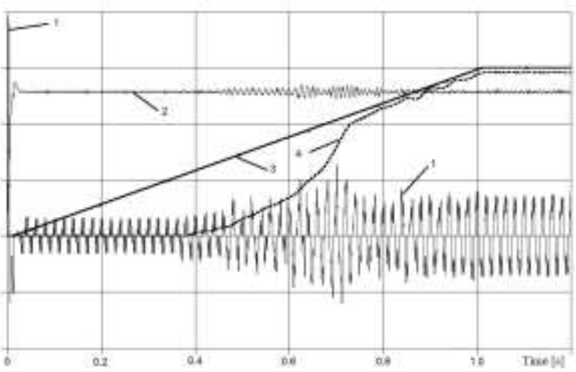

Fig. 3: Time domain simulation results in the presence of L_d from the time moment of FC power supply being turned on until the IM reaches the steady-state operating mode (@ time 1.0 s) at an output AVSI voltage frequency of 50 Hz

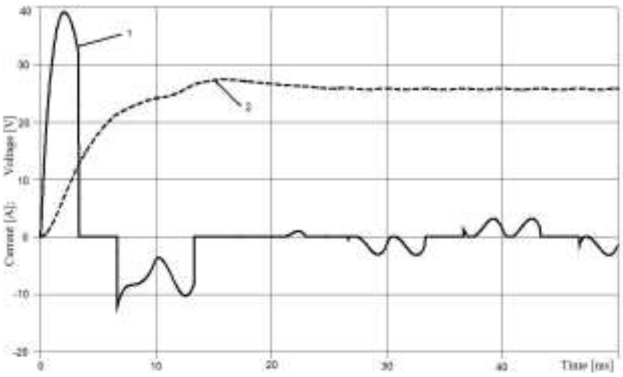

Fig. 4: Time domain simulation results in the presence of L_d. Initial start-up of the FC (first section of the process, shown in Figure 3)

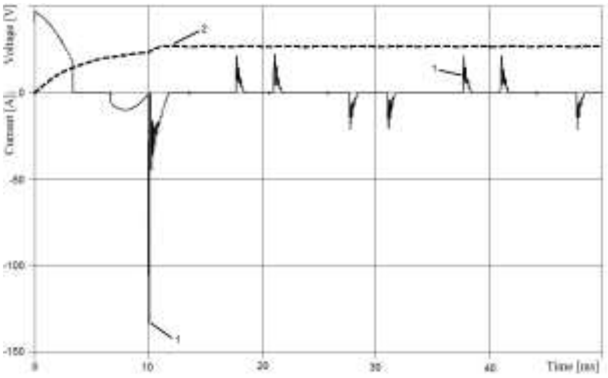

Fig. 5: Time domain simulation results in the absence of L_d. Initial start-up of the FC

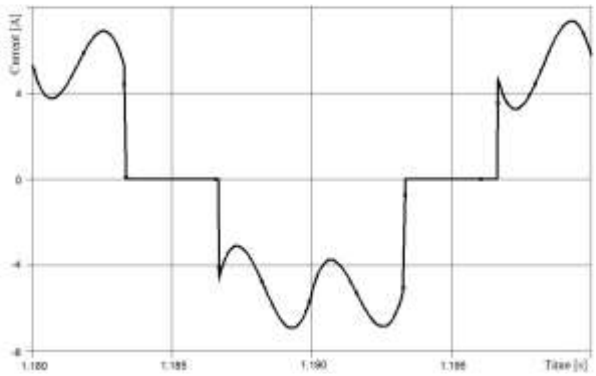

Fig. 6: Time domain simulation results for the input current (magnitude 7.348 A) consumed by the phase of the FC from the grid in steady-state mode after the completion of the acceleration of the IM in the presence of L_d

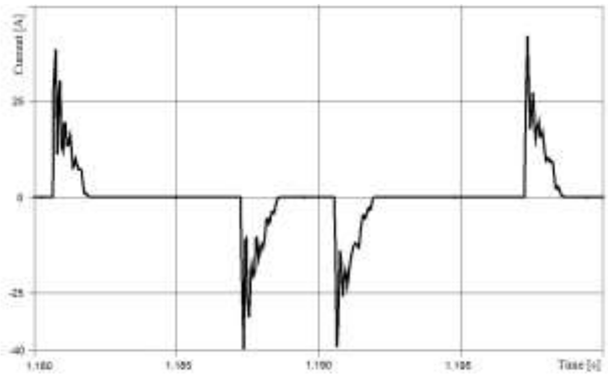

Fig. 7: Time domain simulation results for the input current (magnitude 44.089 A) consumed by the phase of the FC from the grid in steady-state mode after the completion of the acceleration of the IM in the absence of L_d

Peak values of inrush current consumed by the phase of the FC of different power and the times of reaching the maximums are given in Table 6 in order to assess their time difference. Note that the value of the peak inrush current weakly depends on the phase of the input voltage at the moment of turning on the FC. The times of reaching the peak values (maximums) by the current in all cases are so close that the worst case can be considered by accepting the occurrence of peak inrush current for different FCs as simultaneous.

Let, for example, grid voltage be simultaneously supplied to the input of those FCs to outputs of which the following loads are connected: one IM of 1.5 kW, six IMs of 0.75 kW, and nine IMs of 0.37 kW. The total installed shaft power of the supplied IMs in this case will be 9.33 kW. It is easy to calculate that the total input peak current consumed by the one phase of the FCs above mentioned when they are turned on simultaneously will be 352 A, which exceeds the rated RMS output current of the UPS by 8.8 times. It is known that immediately before the failure of the UPS, peaks of current consumption up to 10 times the rate were recorded. When 25 FCs with connected to each one IM of 0.37 kW shaft power are turned on simultaneously, the total installed power of IMs is 9.25 kW, and the total inrush peak current is 625 A, which is 15.6 times higher than the rated RMS output current of the UPS. On the other hand, if grid voltage is simultaneously supplied to the input of those FCs to outputs of which the following loads are connected: one IM of 7.5 kW, one IM of 1.5 kW, one IM of 0.37 kW (total installed shaft power of the supplied IMs in this case is 9.37 kW), then the total inrush peak current will be 205 A, which is only 5.1 times higher than the rated RMS output current of the UPS.

Table 5. Input current consumed by the FC phase simulation results for IMs of different rated shaft power

Name and units of characteristic or parameter	Value		
Rated power of the IM being connected, kW	0.37	0.75	7.5
Peak voltage across C_d terminals during charging, V	575.462	542.402	644.729
Peak inrush current when charging C_d through a precharge resistor R, A	18.401	25.001	147.618
Peak inrush during final charging of C_d through the contactor shunting the precharge resistor R, A	-7.967	-5.817	-145.116
Peak input current during the frequency acceleration of the IM, A	-6.580	8.645	-42.426
Steady-state mode input current amplitude after completion of acceleration of the IM, A	4.342	-8.649	31.912

Table 6. Peak values of inrush current consumed by the phase of the FC from the grid

Rated power of the IM being connected, kW	Peak inrush current when charging C_d through a precharge resistor R	Time to reach maximum, ms	Instantaneous current value @ time moment 2.07 ms
7.5	147.618	2.035	147.580
1.5	39.131	2.070	39.131
0.75	25.001	2.200	24.885
0.37	18.103	1.675	17.560

4 Conclusion

As shown by the results of the computer simulation, the peak value of the inrush phase current consumed by the FC from the grid is observed during the C_d charging process. The presence of L_d inductance should be recognized as very useful and desirable for lower-power and medium-power FCs, since it has a strong limiting effect on the peak and amplitude values of the input current consumed by the FC, and also has a beneficial effect on the harmonic composition of the input current, improving the electromagnetic compatibility of the FC. During the process of initially starting up a group of FCs, the currents consumed by the phases can reach values dangerous for the UPS power semiconductors, exceeding the declared overload capacity several times, although shorter-term. Actions must be taken to ensure that the peak currents consumed by individual FCs do not occur at the same time. Without any doubt, one must also remember that the current through the semiconductor devices of each FC must not exceed the safety limits established for them, [19].

References:

[1] Pustovetov M. Yu., Determination of the Sufficient Inductance of AC Line Reactor at the Input of Frequency Converter, *Journal of Modeling and Optimization*, Vol. 11, No. 1, 2019, pp. 25-29, https://doi.org/10.32732/jmo.2019.11.1.25.

[2] Kabalyk Iu., "A novel method to torque ripples reduction of induction motors with dual stator winding, " *2021 II International Scientific Conference on Advances in Science, Engineering and Digital Education (ASEDU-II-2021)*, Krasnoyarsk, Russia, 2022. p. 60019, https://doi.org/10.1063/5.0104713.

[3] Goolak S., *An Improvement of the Induction Traction Motor's Mathematical Model at Asymmetry of Stator Windings*, Bentham Science Publishers Pte. Ltd. Singapore, 2023, pp. 46-77, https://doi.org/10.2174/9789815124309123010008.

[4] Chalangar H., Ould-Bachir T., Sheshyekani K., Mahseredjian J., Methods for the Accurate Real-Time Simulation of High-Frequency Power Converters, *IEEE Transactions on Industrial Electronics*, Vol. 69, No. 9, 2022, pp. 9613-9623, https://doi.org/10.1109/TIE.2021.3114706.

[5] Akroum H., Kidouche M., Aibeche A., Scalar Control of Induction Motor Drives Using dSPACE DS1104, *International Journal of Electrical Engineering and Computer Science (EEACS)*, Vol. 1, 2019, pp. 90-95. [Online]. https://www.wseas.com/journals/eeacs/2019/2019-014.pdf (Accessed Date: March 5, 2024).

[6] Goolak S., Riabov I., Petrychenko O., Kyrychenko M., Pohosov O. The simulation model of an induction motor with consideration of instantaneous magnetic losses in steel, *Advances in Mechanical Engineering*, Vol. 17, No. 2, 2025, pp. 1-29, https://doi.org/10.1177/16878132251320236.

[7] Darimbaeva N., Mustafin M., Almuratova N., Zhauyt A., Development of a mathematical model of frequency controlled induction electric drive, *Journal of Vibroengineering*, Vol. 23, Iss. 8, 2021, pp. 1833-1844, https://doi.org/10.21595/jve.2021.22051.

[8] Thamizharasan V., Karthikkumar M., Generalized Scalar PWM Approach for Three-Phase Voltage-Source Inverter Fed AC Drive, *International Journal of Electrical Engineering and Computer Science*, Vol. 5, 2023, pp. 123-128, http://dx.doi.org/10.37394/232027.2023.5.13.

[9] Muhammed Fazlur Rahman, Sanjeet K. Dwivedi, *Modeling, Simulation and Control of Electrical Drives*, The Institution of Engineering and Technology, 2019. https://doi.org/10.1049/PBCE118E.

[10] Kellner J., Prazenica M., Method of elimination inrush current after connection of high input DC voltage, *WSEAS Transactions on Power Systems*, Vol. 15, 2020, pp. 110-115. http://dx.doi.org/10.37394/232016.2020.15.13

[11] Ozguc M. K., Ipek E., Aras K., Erhan K., Comprehensive Analysis of Pre-Charge Sequence in Automotive Battery Systems, *Transactions on Environment and Electrical Engineering*, Vol. 4, No. 1, 2021. http://dx.doi.org/10.22149/teee.v4i1.136.

[12] SIEMENS SIMOVERT MASTERDRIVES. Vector Control. Inverter (DC-AC) Compact Type. *Operating Instructions*, [Online]. https://adegis.com/media/asset/589c1fc1b6ff59a12774e8ef676308cc98e6a985f2e6dcae0e89809a2d68b30e.pdf (Accessed Date: March 5, 2024).

[13] Munari B., Schneer A., How to Design a Precharge Circuit for Hybrid and Electric Vehicle Applications. *Technical White Paper. Sensata Technologies*, [Online]. https://www.sensata.com/sites/default/files/a/sensata-how-to-design-precharge-circuits-evs-whitepaper.pdf (Accessed Date: March 5, 2024).

[14] Anandh S., Vijayan S., Paramasivam S. Bench Marking of Alternate Soft-charging Circuits for Variable-frequency Drives, *Research Journal of Applied Sciences, Engineering and Technology*, Vol. 10, No. 8, 2015, pp. 871-881. http://dx.doi.org/10.19026/rjaset.10.2442.

[15] KEB COMBIVERT F4-C. *Reference Manual*, [Online]. https://adegis.com/media/asset/e17e471f3973f3fb7e15888e9d21fc1786bf4ae14c750181d86b6e234dfeb64e.pdf (Accessed Date: March 5, 2024).

[16] ACS 300 Frequency Converters for Speed Control of 0.55 to 11 kW Squirrel Cage Motors. *User's Manual*, [Online]. https://www.otomasyonavm.com/p-pdf/p-abb/abb-acs-300-user-manual-eng.pdf (Accessed Date: March 5, 2024).

[17] Kalenteridis V., Agorastou Z., Siskos S., "A soft start-up technique for inrush current limitation in DC-DC converters," *2019 Panhellenic Conference on Electronics & Telecommunications (PACET)*, Volos, Greece, 2019. pp. 1-4, https://doi.org/10.1109/PACET48583.2019.8956278.

[18] Salcone M., Bond J., "Selecting film bus link capacitors for high performance inverter applications," *2009 IEEE International Electric Machines and Drives Conference*, Miami, FL, USA, 2009, pp. 1692-1699, https://doi.org/10.1109/IEMDC.2009.5075431

[19] Nerubatskyi V., Plakhtii O., Hordiienko D., Mykhalkiv S., Ravlyuk V., A Method for Calculating the Parameters of the Sine Filter of the Frequency Converter, Taking into Account the Criterion of Starting Current Limitation and Pulse-Width Modulation Frequency, *Eastern-European Journal of Enterprise Technologies (EEJET)*, No. 1 (8 (109)), 2021, pp. 6-16, https://doi.org/10.15587/1729-4061.2021.225327.

Contribution of Individual Authors to the Creation of a Scientific Article (Ghostwriting Policy)

The author equally contributed to the present research, at all stages from the formulation of the problem to the final findings and solution.

Sources of Funding for Research Presented in a Scientific Article or Scientific Article Itself

No funding was received for conducting this study.

Conflict of Interest

The author has no conflicts of interest to declare.

Creative Commons Attribution License 4.0 (Attribution 4.0 International, CC BY 4.0)

This article is published under the terms of the Creative Commons Attribution License 4.0 https://creativecommons.org/licenses/by/4.0/deed.en_US